Eur Radiol (2009) 19: 2663–2671
DOI 10.1007/s00330-009-1451-1

F. De Keyzer
V. Vandecaveye
H. Thoeny
F. Chen
Y. Ni
G. Marchal
R. Hermans
S. Nuyts
W. Landuyt
H. Bosmans

Dynamic contrast-enhanced and diffusion-weighted MRI for early detection of tumoral changes in single-dose and fractionated radiotherapy: evaluation in a rat rhabdomyosarcoma model

Received: 3 December 2008
Accepted: 17 April 2009
Published online: 6 June 2009

F. De Keyzer (✉) · V. Vandecaveye · F. Chen · Y. Ni · G. Marchal · R. Hermans · H. Bosmans
Department of Radiology,
University Hospitals Leuven,
Herestraat 49,
3000 Leuven, Belgium
e-mail: Frederik.DeKeyzer@uz.kuleuven.be
Tel.: +32-16-347755
Fax: +32-16-343765

H. Thoeny
Institute of Diagnostic,
Interventional and Pediatric Radiology,
University and Inselspital,
Bern, Switzerland

S. Nuyts
Department of Radiotherapy,
University Hospitals Leuven,
Leuven, Belgium

W. Landuyt
Lab Experimental Radiotherapy,
Catholic University of Leuven (KUL),
Leuven, Belgium

Abstract We aimed to examine different intratumoral changes after single-dose and fractionated radiotherapy, using diffusion-weighted (DW) and dynamic contrast-enhanced (DCE) MRI in a rat rhabdomyosarcoma model. Four WAG/Rij rats with rhabdomyosarcomas in the flanks received single-dose radiotherapy of 8 Gy, and four others underwent fractionated radiotherapy (five times 3 Gy). In rats receiving single-dose radiotherapy, a significant perfusion decrease was found in the first 2 days post-treatment, with slow recuperation afterwards. No substantial diffusion changes could be seen; tumor growth delay was 12 days. The rats undergoing fractionated radiotherapy showed a similar perfusion decrease early after the treatment. However, a very strong increase in apparent diffusion coefficient occurred in the first 10 days; growth delay was 18 days. DW-MRI and DCE-MRI can be used to show early tumoral changes induced by radiotherapy. Single-dose and fractionated radiotherapy induce an immediate perfusion effect, while the latter induces more intratumoral necrosis.

Keywords Diffusion-weighted MRI · Dynamic contrast-enhanced MRI · Experimental tumor model · Radiotherapy · Necrosis

Introduction

An ever increasing number of antitumoral therapies are nowadays being researched or already clinically applied. Conformal and intensity-modulated (IM) radiotherapy (RT) have found widespread use in the curative or (neo) adjuvant setting, often combined with chemotherapy. Combinations of RT with specific antivascular treatments or vascular targeting agents are under investigation [1]. Although fractionated RT is most commonly used, single-dose RT schemes are still used in the palliative setting, to reduce tumor load and patient symptoms [2]. Recently, stereotactic body RT using a high focal dose within a short period has been reported to produce high local control rates. Hypofractionated radiotherapy has therefore gained interest, especially for lung tumors [3]. In these tumors, hypofractionated radiotherapy can also be used with curative intent.

Owing to the large amount of possible treatment schemes, there is an increased need for early, and preferably noninvasive, treatment follow-up. This would enable identification of non- or less-responsive tumors, for which the therapy can then be adapted as early as possible. This may lead not only to a more efficient treatment

scheme, but also to a reduction in treatment-related toxicity.

The anatomical information provided by conventional computed tomography (CT) and magnetic resonance imaging (MRI) examinations is very useful for localization and delineation of tumors. In the context of tumor follow-up, however, treatment response can mainly be assessed based on changes in tumor volumetry, with a successful therapy defined as a strong reduction of tumor size. As a result of the very variable responses depending on treatment type used and the type and localization of the tumor, this volume-based method is of limited value, as it does not provide information on the remaining tissue [4]. Positron emission tomography (PET) is a promising technique, both for detection and follow-up of the metabolic activity of the tumors, but it is hampered by radiotherapy-induced inflammation in the early postradiotherapeutic phase [5].

Diffusion-weighted MRI (DW-MRI) generates image contrast based on the differences in mobility of the water protons in the tissues. This mobility is influenced by the cell density, the amount of vessel structures, and other restrictors of free diffusion [6]. Necrosis is an extreme condition in which a complete disintegration of cell membranes provides a subsequent facilitation of free diffusion that can be visualized with DW-MRI. Tumor perfusion, on the other hand, can be assessed using dynamic contrast-enhanced MRI (DCE-MRI). This type of acquisition can be used to image and quantify the arrival and transit of a contrast agent bolus, yielding a variety of perfusion parameters [7].

The purpose of this study was to describe the changes on DCE-MRI and DW-MRI in tumors after single-dose and fractionated radiotherapy treatment, in correlation with tumor growth. We also compared DCE-MRI and DW-MRI for the early prediction of treatment-induced tumor growth delay.

Materials and methods

Tumor model and study design

The study protocol was approved by the local ethics committee for animal care and use.

Two syngenic R1 rhabdomyosarcoma tumor sections, with a volume of 1 mm^3, were implanted subcutaneously in the flank at the level of the kidneys (one on each side) in 11 rats. The rats in this study were adult male WAG/Rij rats, weighing approximately 280–300 g before implantation. The tumors (n=22) were allowed to grow for 2 weeks postimplantation, reaching an average size of 5.4±2.1 cm^3, after which they received a baseline MRI examination.

Immediately after the baseline examination, four rats (eight tumors) underwent single-dose radiotherapy of 8 Gy and were followed using MRI scans every 2 days for a total period of 14 days. Four other rats (eight tumors) received a fractionated dose of 15 Gy administered in five consecutive sessions of 3 Gy. These rats underwent follow-up MRI at days 2, 4, 7, 11, 18, and 25 after the start of radiotherapy. Tumor volumes were always measured using a caliper before each MR examination. The remaining three rats (six tumors) were used as controls to assess growth evolution of the rhabdomyosarcoma tumors in untreated animals. These control rats did not undergo MRI, but only periodic volumetric caliper measurements in the first 2 weeks after the start of the study.

During the entire study, all rats were kept in a conventional housing facility and given free access to food and water. At the end of the study, all rats were sacrificed.

MRI examination

The rats were examined in a clinical 1.5-T whole body MR system (SonataVision; Siemens, Erlangen, Germany) with a maximum gradient magnitude of 40 mT/m, using a four-channel phased-array wrist coil. To minimize repositioning errors and animal motion, the rats were placed supinely in a plastic holder and initially anesthetized by inhalation of 4% isoflurane in a mixture of 70% oxygen and 30% room air. During the entire examination, the anesthesia was maintained using an inhalation of 2% isoflurane in a mixture of 20% oxygen and 80% room air. In order to maintain body temperature during the examination, the rats were wrapped in towels. Intravenous access for the injection of contrast agent was prepared in a tail vein before the MR examination.

Besides standard anatomical T1- and T2-weighted spin-echo sequences, diffusion-weighted MR images were acquired using a spin-echo echoplanar imaging sequence with the following parameters: 20 slices acquired using a 2.0-mm slice thickness, 0.2-mm intersection gap, field of view of 113.8×130 mm, matrix of 80×128, TR/TE of 3500 ms/124 ms, 4 averages, parallel imaging (generalized autocalibrating partially parallel acquisition, GRAPPA) with a reduction factor of 2, and a resulting voxel size of 1.4×1.0×2.0 mm^3 in an acquisition time of 2 min 24 s. The following ten diffusion-sensitizing gradients were applied along the x-axis of the magnet: b=0, 50, 100, 150, 200, 250, 300, 500, 750, and 1,000 s/mm^2. An example image can be seen in Fig. 1a.

For dynamic contrast-enhanced MR imaging, a 3D T1-weighted fast spoiled gradient-echo sequence (volumetric interpolated breath-hold examination, VIBE) was used to obtain dynamic sets of 20 slices with a slice thickness of 2.0 mm, field of view of 81.3×130 mm^2, matrix of 96×192, TR/TE of 6.97 ms/2.61 ms, 1 average, parallel imaging (GRAPPA) with a reduction factor of 2, and a resulting voxel size of 0.8×0.7×2.0 mm^3 in an acquisition time of 3.7 s per volume of 20 slices. After a baseline of 11

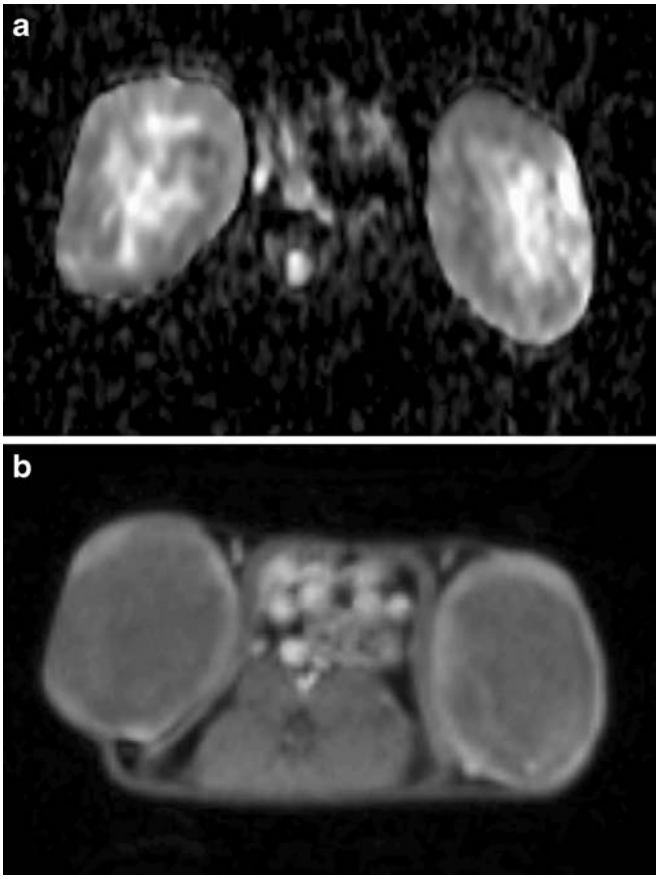

Fig. 1 Examples of an ADC map (**a**) and a DCE-MRI image (**b**), at maximal contrast enhancement, of the same rat before treatment, with bilaterally implanted tumors

volumes, a dose of 0.2 ml of gadodiamide (Omniscan, 0.5 mmol/l of gadolinium; Amersham, Oslo, Norway) was manually injected intravenously during the acquisition of five sets of 20 slices. Thereafter, another 84 VIBE sets of 20 slices were performed to visualize the dynamic enhancement pattern. An example image can be seen in Fig. 1b.

Data analysis

Data was processed off-line using BioMap (Novartis, Basel, Switzerland) software.

For the processing of diffusion-weighted images, regions of interest (ROIs) were delineated around the tumor on the images acquired with a *b* value of 0 s/mm^2 (b0 images). This delineation was done on all slices with visible tumor. All individual ROIs were then combined into a single (three-dimensional) ROI that included the complete tumor. These ROIs were automatically copied to the other *b*-value images and the mean signal intensity per *b* value was calculated. Combining the information from the different *b*-value images allowed the calculation of different apparent diffusion coefficients (ADCs). ADCs were calculated for the entire *b*-value series (ADC_{avg}), for low *b* values of 0, 50, and 100 s/mm^2 (ADC_{low}) and for high *b* values of 500, 750, and 1,000 s/mm^2 (ADC_{high}), identical to the study by Thoeny et al. [8].

Similarly, central and peripheral ROIs were delineated on three slices through the center of the tumor using the following rule of thumb: the periphery is less than 5 mm thick, while the center is the collection of tissue that is more than 8 mm from the edge of the tumor.

For the DCE-MRI images, regions of interest were delineated in the baseline images and copied over the entire dynamic series. Central and peripheral ROIs were again delineated following the same procedure as in the DW-MRI examinations. The dynamic signal intensity curves were pixel-wise transformed into relative signal intensity curves (contrast–time curves, CTC) by dividing signal intensities of the successive images by the signal intensity on the baseline image. Using these CTC, the following parameters were calculated: the maximal wash-in slope of contrast enhancement (initial slope, IS) and the maximal relative contrast enhancement (contrast peak, C_{peak}).

Detection of statistical changes in diffusion or perfusion parameters during the longitudinal follow-up period was performed using paired two-tailed Student's *t* tests with Bonferroni correction for multiple testing. Changes in tumor volume between the groups of treated rats and the control group were assessed using unpaired two-tailed Student's *t* tests. A *P* value of less than 0.05 was considered significant.

Results

Tumor volume

Volumetry of the control tumors showed an exponential growth reaching 24.1±8.0 cm^3 at day 11 after their inclusion in the study (Fig. 2). At the 14th day, the tumors treated with a single-dose irradiation reached a volume of 13.0±4.6 cm^3, representing a treatment-induced tumor growth delay of 10 days (Fig. 2). In the group of rats treated with a fractionated radiotherapy scheme, the tumors needed 24 days to reach a volume of 16.9±6.0 cm^3. This group showed a tumor growth delay of 18 days (Fig. 2), which was significantly longer than the group of rats treated with single-dose radiotherapy ($P<0.001$).

Whole tumor delineations

The single-dose irradiation resulted in a significant decrease in IS and in C_{peak} by 2 days ($P<0.01$) and persisting lower values until day 8 after the start of treatment (Fig. 3). After 8 days, slow recuperation of IS and C_{peak} occurred with values approximating the baseline values in the same animals after 14 days. The fractionated

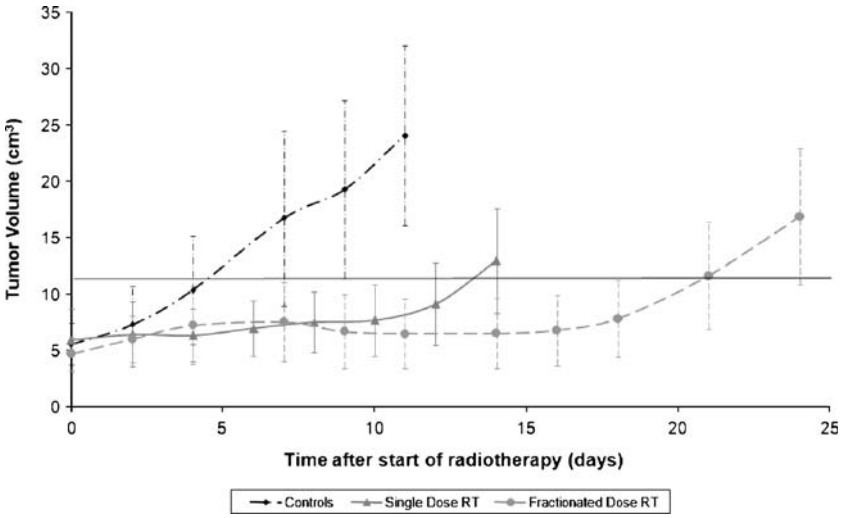

Fig. 2 Evolution of tumor volume over the follow-up period, averaged over all animals for each subgroup. The time difference in tumor doubling time (crossing of the *horizontal line*) indicates the tumor growth delay caused by the different treatments. The tumor growth delay compared with the controls is 10 days for the single-dose and 18 days for the fractionated radiotherapy. *Error bars* ±SD

radiotherapy scheme induced a similar significant decrease ($P<0.01$) in IS and C_{peak} in the early post-treatment period ($P>0.05$ for the comparison of the perfusion parameters of the different treatment groups), and this decrease lasted up to 12 days after the start of the treatment. Recuperation of the perfusion parameters was visible on the next time points with a slightly, however not significantly, increased perfusion (IS and C_{peak}), at 25 days post-treatment when compared with baseline (Fig. 3).

When looking at the diffusion measurements, and more specifically at the ADC_{high} and ADC_{avg} values, no significant changes could be seen in the tumors treated with a single-dose irradiation (Fig. 4) over the entire follow-up period. The ADC_{low} values showed a small increase in the early post-treatment period, but statistical significance was not reached. The fractionated radiotherapy scheme, on the other hand, resulted in a significant and continuous increase in ADC_{high}, ADC_{low}, and ADC_{avg} during the first 10 days after the start of the treatment ($P<0.001$ for all ADC values). During the following 15 days, these values decreased again to reach values about 25% higher than the baseline values.

Central and peripheral tumor areas

In the central tumor areas, IS and C_{peak} decrease significantly in the early post-treatment phase up to 8 days after the start of treatment for both treatments (Fig. 5). Afterwards, this situation of low perfusion is maintained for the rest of the follow-up period, without substantial changes in IS or C_{peak}. In the periphery, a variable behavior is seen without substantial changes over the entire follow-up period for the single-dose or fractionated radiotherapy.

In the central ROIs, the ADC_{avg}, ADC_{low}, and ADC_{high} values increase significantly ($P<0.01$) in the early post-treatment phase for single-dose and fractionated radiotherapy (Fig. 6). Again, this situation of increased ADC values is maintained in the later follow-up examinations. The peripheral ADC values show similar behavior as those of the entire tumor delineations, with significant increases in the early phase ($P<0.001$) and a return to baseline values later on (Fig. 6).

Functional information in combination with tumor volumetry

When combining the volumetric and the functional information, it can be seen that the recuperation of the perfusion parameters in a single-dose irradiation scheme precedes the onset of renewed volume increase by 2 days. For the fractionated radiotherapy group, however, a significant volume increase was only seen 4 days after the recuperation of both the perfusion and the diffusion parameters.

Discussion

A few studies have indicated that tumor size before treatment and, more importantly, volume regression early after radiotherapy can accurately assess and even predict treatment outcome [9–12]. However, volume reduction is not always characteristic for successful treatment in all tumor types and locations. In the current rat rhabdomyosarcoma model, no significant volume reduction can be seen after radiotherapy treatment (current study) or after combretastatin A-4 phosphate [13]. Instead, a successful treatment, expressed in terms of growth delay, is characterized by a decrease in perfusion and/or an increase of the necrotic fraction of the tumor. These intratumoral changes necessitate a, preferably noninvasive, imaging method that allows imaging of the entire tumor, such as DW-MRI and DCE-MRI.

In animal brain models, DW-MRI was able to identify development of necrosis due to successful treatment by an

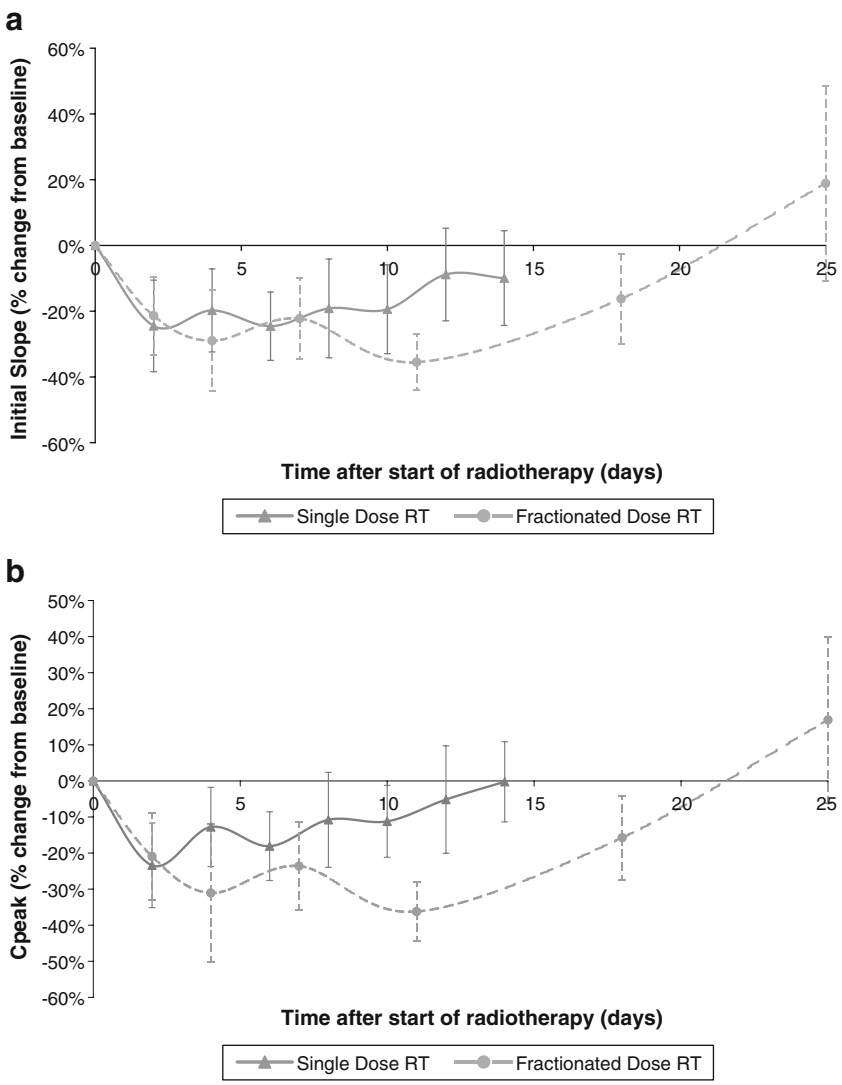

Fig. 3 Evolution of perfusion parameters of the entire tumor volumes (averaged values over all animals in the subgroup) after treatment with single-dose and fractionated radiotherapy. A significant decrease is seen in the early post-treatment phase in initial slope (**a**) and C_{peak} (**b**) for single-dose and fractionated radiotherapy. This initial decrease disappears in the later follow-up time points, with the fastest return in the single-dose radiotherapy group. *Error bars* ±SD

increase in ADC values [14–16]. After radiotherapy in human brain tumors, a similar increase in ADC values was found in almost all responding lesions, but not in the nonresponders [17, 18]. Tomura et al. found an ADC increase of about 35% in a group of 39 patients, treated with one to five doses of stereotactic irradiation. The group of responders in that study had a significantly higher increase in ADC value than the nonresponders. The current study also showed a significant increase in ADC in the group of rats treated with fractionated irradiation, on average 60–80% depending on the ADC calculation used. The rhabdomyosarcoma used in this study is a very aggressive tumor, but is also very susceptible to treatments targeting the tumor vasculature, as depicted by Thoeny et al. [8]. This explains the huge increase in ADC, contributing to formation of necrosis. However, the tumors treated with single-dose radiotherapy only showed a small increase in ADC_{low}, but not in ADC_{high} and ADC_{avg}. The latter observation indicates that the direct necrosis formation seems minimal in this setting of single-dose radiotherapy. The small, but noticeable, increase in ADC_{low} probably indicates a vascular effect of the treatment [19].

When looking at the ADC values of the center and periphery separately, a clear difference can be seen. All calculated ADC values in the center increase after the start of treatment in both the fractionated dose and single-dose radiotherapy settings, corresponding to necrosis formation, and remain elevated in the following days. The fractionated dose radiotherapy induced a stronger ADC increase than the single-dose treatment. In the periphery, a strong increase can be seen in the fractionated radiotherapy for all calculated ADC values. After 10 days, however, the ADC values return to baseline, most likely due to regrowth of the tumor from the periphery.

Some studies have already described the use of DCE-MRI for examining the effect of fractionated radiotherapy on the tumor vasculature [20–22]. In a rat tumor model, Ceelen et al. used a macromolecular contrast

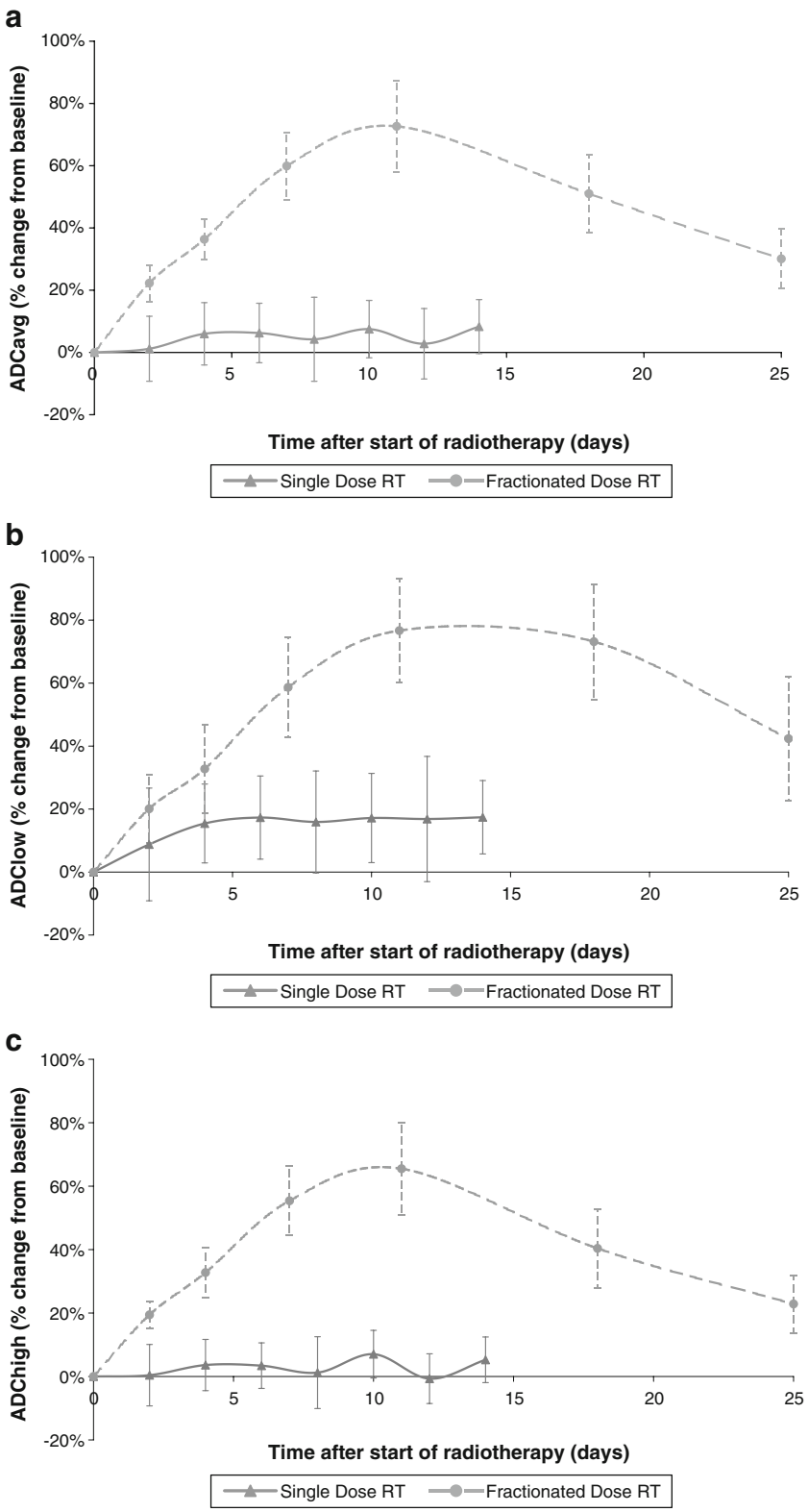

Fig. 4 Diffusion changes of the entire tumor volumes after treatment with single-dose or fractionated radiotherapy. In the single-dose treatment group, no changes in ADC_{avg} (**a**) or ADC_{high} (**c**) can be seen over the entire follow-up period, although there is a small increase in ADC_{low} (**b**). In the group with fractionated radiotherapy, however, a very strong increase in all ADC values is evident in the first 10 days after the start of radiotherapy, with partial return to baseline ADC values afterwards. *Error bars* ±SD

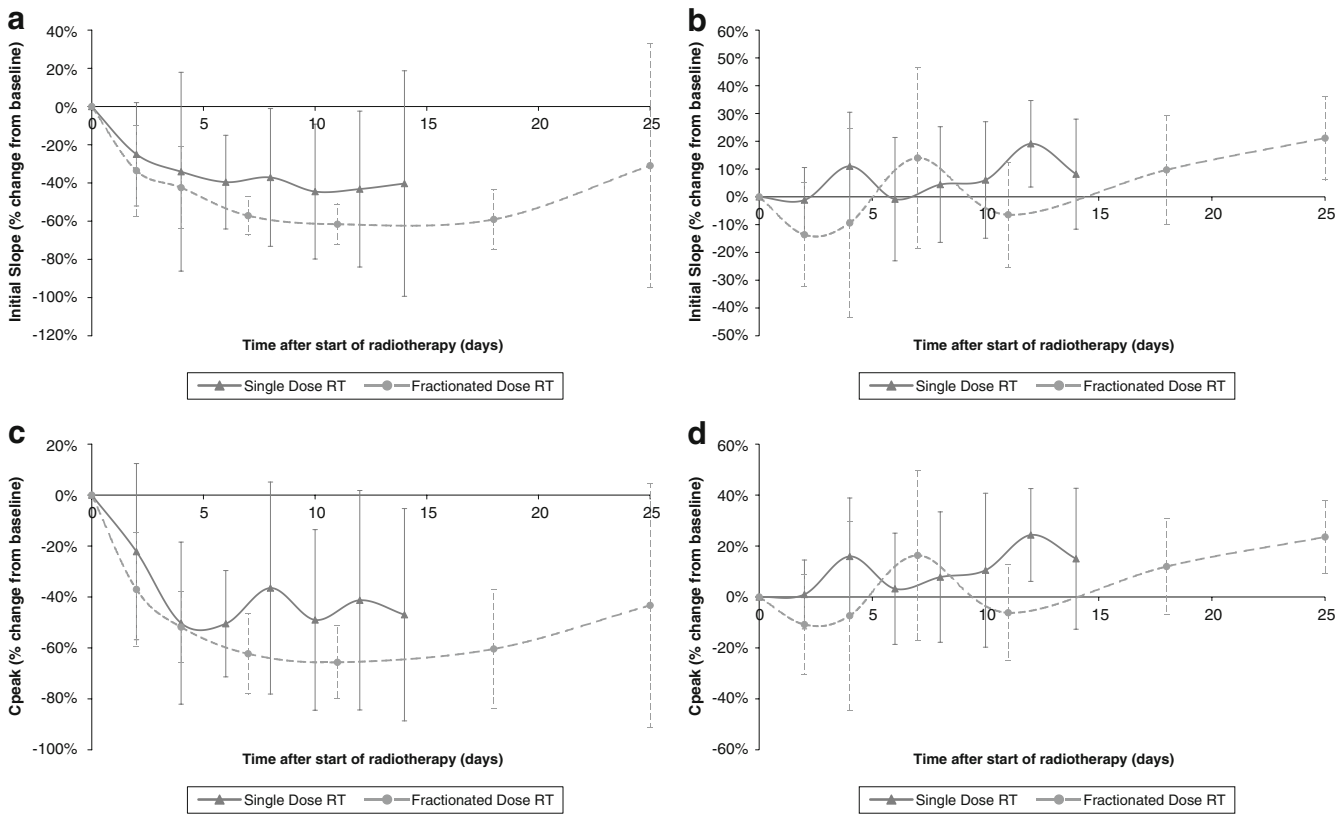

Fig. 5 Perfusion changes in the central (*left column*) and peripheral (*right column*) tumor areas after treatment with single-dose and fractionated radiotherapy. In the central areas, a clear decrease is evident for initial slope (**a**) and C_{peak} (**c**) in the first days post-treatment and persists for the entire follow-up period. The perfusion parameters in the periphery (initial slope (**b**) and C_{peak} (**d**)) show variable behavior. *Error bars* ±SD

agent and found that K_{trans} decreased significantly after five irradiations of 5 Gy each [20]. On the other hand, Kobayashi et al. found no substantial changes in K_{trans} in a mouse model with similar fractionated irradiation schemes, but they did find a significant decrease in K_{trans} when single-dose radiotherapy was applied [21]. The difference between these studies could be due to a different choice of follow-up time points, 5 days and 48 h after radiotherapy, respectively. Horsman et al. also found that single-dose radiotherapy was superior to the same dose in fractionated irradiation [22]. The current study showed a significant decrease of perfusion in the first days after the start of treatment with recuperation or regrowth afterwards, corresponding with the previous studies. However, the immediate perfusion decrease of both treatments was very similar in this tumor model, and a faster recuperation was found in single-dose radiotherapy. This can probably be attributed to a more aggressive tumor type with fast regrowth, to the lower overall radiation dose, or to the smaller contrast agent molecules used in the current study.

For both treatment settings, the periphery of the tumors did not show a strong perfusion reduction. The central tumor parts, on the other hand, showed an important decrease in perfusion which persisted in the following days, especially with fractionated irradiation, indicative of necrosis. This was confirmed after excision.

Although the early (in the first few days) DCE-MRI changes can be used to indicate that the treatment has an effect, no information is provided on the expected tumor growth delay. Both treatments have similar DCE-MRI changes, but still present with strongly different tumor growth delays. The different growth delays of single-dose versus fractionated irradiation can, however, be predicted by the different DW-MRI responses in the first days after the start of treatment, with a strong ADC increase indicative of a longer tumor growth delay.

A limitation of the study is that relatively few rats were included in the different treatment groups, and that they were followed for only a couple of weeks postradiotherapy. As a result of the difference in growth between the two tumors in the same animal, there is a larger intratumoral difference at the start of treatment when compared with studies employing a single tumor per rat. However, low intersubject response variability was found in the rats undergoing the same treatment,

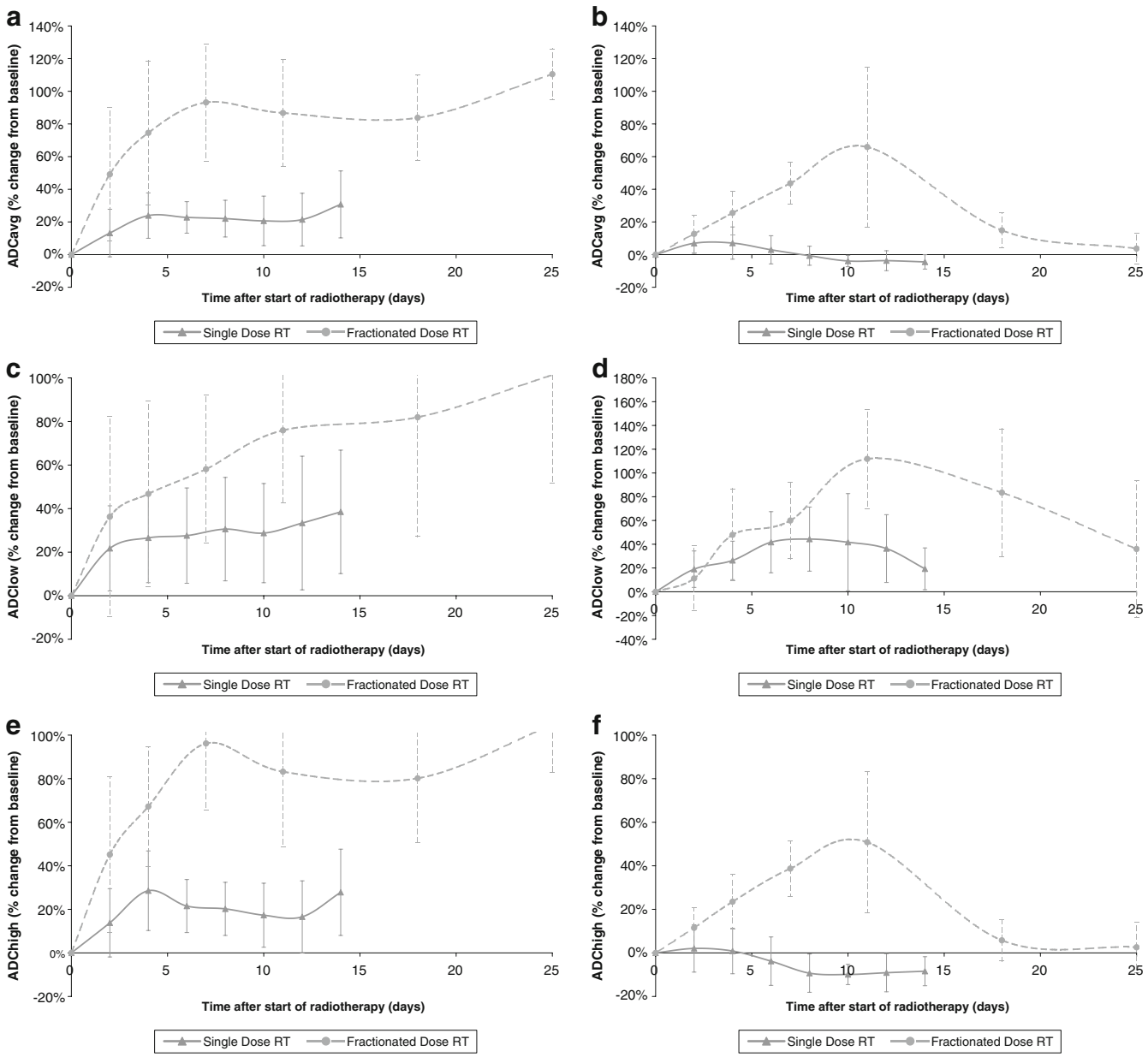

Fig. 6 Diffusion changes in the central (*left column*) and peripheral (*right column*) tumor areas after treatment with single-dose or fractionated radiotherapy. In the central areas, the single-dose and the fractionated radiotherapy groups display a significant increase in ADC_{avg} (**a**), ADC_{low} (**c**), and ADC_{high} (**e**), with the stronger increase found in the fractionated radiotherapy group. These ADC increases in the central tumor areas persist in the later follow-up examinations. The ADC values in the central ROIs are very similar to those of the entire tumor delineations, with significant increases in ADC_{avg} (**b**), ADC_{low} (**d**), and ADC_{high} (**f**) in the group of rats treated with fractionated radiotherapy in the first 10 days post-treatment. In the peripheral areas, the single-dose radiotherapy group does not show substantial changes in ADC_{avg} or ADC_{high}, but a small increase in ADC_{low}. The changes in the peripheral tumor areas all return to baseline values in the follow-up examinations

indicating the homogeneity of the tumor model in its response to radiotherapy. Also, as the tumor model grows very fast, the animal studies can be set up very quickly, but this has the downside that the maximal tumor size, as set by the ethical committee, is reached earlier, and subsequently that follow-up periods are limited. Another downside of the used tumor model is that it probably does not closely mimic the real clinical situation, because the tumors are quite big and have a large central hypoperfused area before the start of the treatment. The current difference found between single-dose and fractionated radiotherapy will probably be less obvious in a clinical situation, but this needs to be examined in a future study.

Conclusion

DW-MRI and DCE-MRI were able to assess the intratumoral changes induced by single-dose or fractionated radiotherapy in this rat tumor model. Single-dose radiotherapy induced a strong immediate perfusion decrease, but only limited necrosis and a moderate tumor growth delay. On the other hand, fractionated radiotherapy showed a similar, albeit less strong, immediate perfusion decrease but a very strong necrosis formation and a longer tumor growth delay. While DCE-MRI could be used to examine the immediate treatment-induced effects, DW-MRI provided a better correlation with tumor growth delay. In the current tumor model, DW-MRI therefore seems a better early predictor of radiotherapy-induced tumor growth stop. Future studies comparing different radiotherapy settings or a combination of treatments could therefore benefit from using both techniques that can easily be combined in a single MRI examination.

Acknowledgments This work has been partly financially supported by the research grant "Prof. Em. A. L. Baert, Siemens Medical Solutions".

References

1. Senan S, Smit EF (2007) Design of clinical trials of radiation combined with antiangiogenic therapy. Oncologist 12:465–477
2. Hartsell WF, Scott CB, Bruner DW et al (2005) Randomized trial of short- versus long-course radiotherapy for palliation of painful bone metastases. J Natl Cancer Inst 97:798–804
3. Onimaru R, Fujino M, Yamazaki K et al (2007) Steep dose–response relationship for stage I non-small-cell lung cancer using hypofractionated high-dose irradiation by real-time tumor-tracking radiotherapy. Int J Radiat Oncol Biol Phys 70:374–381
4. Stroobants S, Goeminne J, Seegers M et al (2003) 18FDG-positron emission tomography for the early prediction of response in advanced soft tissue sarcoma treated with imatinib mesylate (Glivec). Eur J Cancer 39:2012–2020
5. Grégoire V, Bol A, Geets X et al (2006) Is PET-based treatment planning the new standard in modern radiotherapy? The head and neck paradigm. Semin Radiat Oncol 16:232–238
6. Le Bihan D (1995) Molecular diffusion, tissue microdynamics and microstructure. NMR Biomed 8:375–386
7. Padhani AR, Husband JE (2001) Dynamic contrast-enhanced MRI studies in oncology with an emphasis on quantification, validation and human studies. Clin Radiol 56:607–620
8. Thoeny HC, De Keyzer F, Chen F et al (2005) Diffusion-weighted MR imaging in monitoring the effect of a vascular targeting agent on rhabdomyosarcoma in rats. Radiology 234:756–764
9. Mayr NA, Magnotta VA, Ehrhardt JC et al (1996) Usefulness of tumor volumetry by magnetic resonance imaging in assessing response to radiation therapy in carcinoma of the uterine cervix. Int J Radiat Oncol Biol Phys 35:915–924
10. Allen SD, Padhani AR, Dzik-Jurasz AS et al (2007) Rectal carcinoma: MRI with histologic correlation before and after chemoradiation therapy. Am J Radiol 188:442–451
11. Hatano K, Sekiya Y, Araki H et al (1999) Evaluation of the therapeutic effect of radiotherapy on cervical cancer using magnetic resonance imaging. Int J Radiat Oncol Biol Phys 45:639–644
12. van de Bunt L, van der Heide UA, Ketelaars M et al (2006) Conventional, conformal and intensity-modulated radiation therapy treatment planning of external beam radiotherapy for cervical cancer: the impact of tumor regression. Int J Radiat Oncol Biol Phys 64:189–196
13. Thoeny HC, De Keyzer F, Chen F et al (2005) Diffusion-weighted magnetic resonance imaging allows noninvasive in vivo monitoring of the effects of combretastatin A-4 phosphate after repeated administration. Neoplasia 7:779–787
14. Seierstad T, Folkvord S, Roe K et al (2007) Early changes in apparent diffusion coefficient predict the quantitative antitumoral activity of capecitabine, oxaliplatin, and irradiation in HT29 xenografts in athymic nude mice. Neoplasia 9:392–400
15. Chenevert TL, McKeever PE, Ross BD (1997) Monitoring of early response of experimental brain tumors to therapy using diffusion MRI. Clin Cancer Res 3:1457–1466
16. Stegman LD, Rehemtulla A, Hamstra DA et al (2000) Diffusion MRI detects early events in the response of a glioma model to the yeast cytosine deaminase gene therapy strategy. Gene Ther 7:1005–1010
17. Mardor Y, Pfeffer R, Spiegelmann R (2003) Early detection of response to radiation therapy in patients with brain malignancies using conventional and high b-value diffusion-weighted magnetic resonance imaging. J Clin Oncol 21:1094–1100
18. Tomura N, Narita K, Izumi J et al (2006) Diffusion changes in a tumor and peritumoral tissue after stereotactic irradiation for brain tumors: possible prediction of treatment response. J Comput Assist Tomogr 30:496–500
19. Thoeny HC, De Keyzer F, Vandecaveye V et al (2005) Effect of vascular targeting agent in rat tumor model: dynamic contrast-enhanced versus diffusion-weighted MR imaging. Radiology 237:492–499
20. Ceelen W, Smeets P, Backes W et al (2006) Noninvasive monitoring of radiotherapy-induced microvascular changes using dynamic contrast enhanced magnetic resonance imaging (DCE-MRI) in a colorectal tumor model. Int J Radiat Oncol Biol Phys 64:1188–1196
21. Kobayashi H, Reijnders K, English S et al (2004) Application of a macromolecular contrast agent for detection of alterations of tumor vessel permeability induced by radiation. Clin Cancer Res 10:7712–7720
22. Horsman MR, Nielsen T, Ostergaard L et al (2006) Radiation administered as a large single dose or in a fractionated schedule: role of the tumour vasculature as a target for influencing response. Acta Oncol 45:876–880